Biosensors and Bioelectronics 58 (2014) 40–47

Contents lists available at ScienceDirect

Biosensors and Bioelectronics

journal homepage: www.elsevier.com/locate/bios

DNA-AuNPs based signal amplification for highly sensitive detection of DNA methylation, methyltransferase activity and inhibitor screening

Xiaoying Jing [a], Xianqing Cao [a], Li Wang [a], Tian Lan [b], Yiyan Li [c], Guoming Xie [a,*]

[a] Key Laboratory of Laboratory Medical Diagnostics of Education, Department of Laboratory Medicine, Chongqing Medical University, No. 1 Yi Xue Yuan Road, Chongqing 400016, PR China
[b] Department of Chemistry, University of Illinois at Urbana-Champaign, 600 South Mathews Avenue, Urbana, IL 61801, USA
[c] Nevada Nanotechnology Center, College of Engineering, University of Nevada, Las Vegas, NV 89154-4026, USA

ARTICLE INFO

Article history:
Received 6 November 2013
Received in revised form
13 February 2014
Accepted 14 February 2014
Available online 25 February 2014

Keywords:
DNA methylation
Methyltransferase activity
DNA-AuNPs amplification unit
Methylene blue
Inhibitor screening
Electrochemical assay

ABSTRACT

A sensitive and selective electrochemical method was developed for the detection of DNA methylation, determination of DNA methyltransferase (MTase) activity and screening of MTase inhibitor. Methylene blue (MB) was employed as electrochemical indicator and DNA-modified gold nanoparticles (AuNPs) were used as signal amplification unit because the DNA strands in this composite have strong adsorption ability for MB. First, the thiolated single-stranded DNA S1 was self-assembled on gold electrode, hybridization between the lower portion of DNA S1 and its complementary DNA S2 formed an identical double-stranded tetranucleotide target sequence for both DNA adenine methylation (Dam) MTase and methylation-resistant endonuclease Mbo I, then the upper portion of DNA S1 was hybridized with its complementary DNA S3 modified on AuNPs to bring the DNA S3-AuNPs amplification units onto the electrode. The DNA S1/S2/S3-AuNPs bioconjugate has lots of DNA strands, and they can adsorb abundant MB. Mbo I endounuclease could not cleave the identical target sequence after it was methylated by Dam MTase. On the contrary, the sequence without methylation could be cleaved, which would decrease the amount of adsorbed MB. The presence of redox-active MB was detected electrochemically by differential pulse voltammetry (DPV). Thus, the activity of Dam MTase and methylation status were sensitively converted to the DNA S3-AuNPs amplified DPV signals. The DPV signal demonstrated a linear relationship with logarithm of Dam concentration ranging from 0.075 to 30 U/mL, achieving a detection limit of 0.02 U/mL ($S/N=3$). Also, screening of Dam MTase inhibitor 5-fluorouracil was successfully investigated using this fabricated sensor.

1. Introduction

Epigenetics is known as heritable changes in gene expression that are not caused by changes in DNA sequences (Holliday, 1987). It mainly contains three systems, DNA methylation, RNA-associated silencing and histone modification (Egger et al., 2004). DNA methylation is the most well-known epigenetic modification, and it plays a significant regulatory role in both prokaryotes and eukaryote (Heithoff et al., 1999; Robertson, 2005). Aberrant DNA methylation influences the interaction between DNA and protein, and alert gene expression, which is associated with a wide range of diseases (Heithoff et al., 1999; Jones and Baylin, 2002), even tumor occurrence and tumor growth (Baylin and Ohm, 2006; Jeltsch, 2002; Robertson and Wolffe, 2000; Shames et al., 2007; Simon, 2005).

DNA methylation is a process carried out by DNA methyltransferase (MTase), which catalyzes methyl group transfer from the donor S-adenosyl-L-methionine (SAM) to the target adenine or cytosine and produces S-adenosyl-L-homocysteine (AdoHcy) and methylated DNA (Adams, 1990; Frauer and Leonhardt, 2009; Grandjean et al., 2007; Horton et al., 2006; Song et al., 2009). The activity of MTase influences DNA methylation level, and the overexpression of DNA MTase in many cancer cells has been confirmed. The abnormity of DNA MTase activity is related to the pathogenesis of acute monocytic leukemia, which provides a useful and new biomarker for interrelated cases (Yan et al., 2011). In addition, the inhibition of MTases may provide a broad spectrum of antimicrobial application (Brueckner and Lyko, 2004; Mashhoon et al., 2006). Due to the importance of MTase in the DNA methylation process, the quantification and activity analysis of DNA MTase are very critical.

So far, a large number of methods have been developed to investigate DNA methylation and DNA MTase activity, such as radioactive labeling (Adams et al., 1991), high-performance liquid

* Corresponding author. Tel./fax: +86 23 68485240.
E-mail address: guomingxie@cqmu.edu.cn (G. Xie).

http://dx.doi.org/10.1016/j.bios.2014.02.035
0956-5663

chromatography (HPLC) (Boye et al., 1992), polymerase chain reaction (PCR) (Eads et al., 1999), electrochemical biosensors (J. Chen et al., 2010), gel electrophoresis (Bergerat et al., 1991), fluorescence method (Zhao et al., 2013), bisulfate treatment (Wan et al., 2007), bioluminescence (Jiang et al., 2012) and colorimetric approaches (Li et al., 2010). Among all these methods, electrochemical biosensors have received an intensive attention due to the advantages of convenience, sensitivity, fast response, low production cost and ease of miniaturization (Baek et al., 2013; X. Chen et al., 2010). For instance, Ai's group employed anti-5-methycytosine antibody and horseradish peroxidase labeled IgG (IgG-HRP) to detect DNA methylation and the activity of DNA MTase with high sensitivity (Wang et al., 2012). In addition, an assay based on methyl binding domain (MBD) proteins and coomassie brilliant blue G250 (CBB-G250) has been designed by them (Yin et al., 2013a). To simplify the detection methods, Li's group developed an electrochemical biosensor to detect DNA methylation and MTase activity based on voltammetric response of electroactive intercalator ($[Ru(NH_3)_6]^{3+}$), which was adsorbed on DNA strands via the electrostatic interaction (Wang et al., 2013). However, the detection limit of this method for DNA MTase was 0.18 U/mL. To better apply DNA MTase to early diagnose interrelated diseases, further improvement on the detection limit for DNA MTase is needed. Moreover, a simple and effective signal amplification system is needed.

As a stable nanomaterial, gold nanoparticles (AuNPs) have excellent biocompability (Cao et al., 2012; Jie et al., 2010; K. Liu et al., 2011; Yin et al., 2011), and can be conjugated with various kinds of biomolecules without affecting their nature and activity. For example, DNA modified AuNPs have been widely used for biosensor (Rosi and Mirkin, 2005) and nanotechnology (Baron et al., 2007; Katz and Willner, 2004). Methylene blue (MB) is an organic dye that has electroactivity, it can interact with DNA by three modes, including electrostatic interaction with the deoxyribose-phosphate backbone, intercalation between base pairs on double-stranded DNA, and specific interaction with exposed guanine residues in single-stranded DNA (Dai et al., 2012; Erdem et al., 2000; Kerman et al., 2002; Zhang and Hu, 2007). Combining MB's properties of electroactivity and capability to interact with DNA strands, it was employed as signal molecules (Lin et al., 2007; Xu et al., 2013).

In this study, we developed a more sensitive electrochemical method for the detection of DNA methylation and DNA MTase activity using DNA-AuNPs amplification. As Scheme 1 shows, this assay based on the electrochemical response of MB, it could accumulate onto the surface of DNA S1/S2/S3-AuNPs bioconjugates-modified gold electrode as an indicator after the Dam and Mbo I recognition site was methylated by Dam MTase and digested by Mbo I restriction endonuclease. DNA Adenine MTase (Dam), catalyzing the N6-adenine methylation in the symmetric tetranucleotide 5′-G-A-T-C-3′, was used as a model MTase (Horton et al., 2006). The endonuclease Mbo I, which identifies the same site (a double-stranded DNA containing 5′-G-A-T-C-3′ palindrome sequence) as Dam MTase, was employed to cleave the unmethylated sites on the double-stranded DNA. Firstly, thiolated DNA S1 was self-assembled onto a gold electrode via Au–S bonding, followed by hybridization with DNA S2 to form double-stranded DNA containing a specific recognition sequence for Dam MTase and methylation-resistant endonuclease Mbo I. DNA S3-AuNPs amplification unit was then successively brought onto the gold electrode surface through hybridization between DNA S3 and the upper portion of DNA S1. The unmethylated DNA hybrid was selectively digested by Mbo I and only a small amount of MB could be adsorbed on the electrode without DNA S3-AuNPs amplification units. So a relatively lower electrochemical signal of MB was achieved. However, after methylation event by Dam MTase, the Mbo I digestion was blocked; thus the DNA S3-AuNPs amplification units remained on the electrode, and lots of MB could accumulate onto the surface of DNA S1/S2/S3-AuNPs bioconjugates modified Au electrode, which resulted in a high electrochemical signal. Therefore, Dam MTase activity and DNA methylation could be sensitively detected through

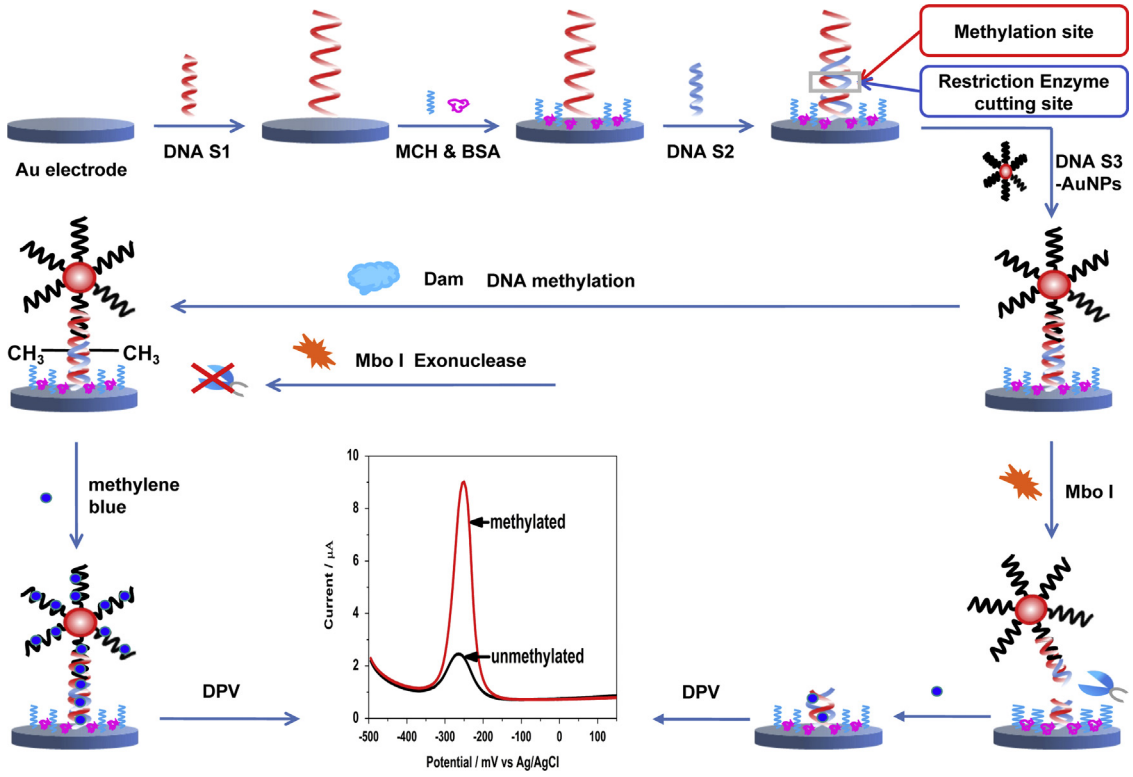

Scheme 1. Schematic representation of the developed method for detection of DNA methylation and assay of DNA methyltransferase activity.

the electrochemical signals, which could be attributed to the powerful amplification effect of the DNA-AuNPs unit. Furthermore, the pharmacological inhibitors of DNA MTase had promising applications for antibiotics and anticancer therapeutics, so the effect of the inhibitor on MTase activity was also investigated, which would provide a sensitive platform for screening DNA MTase inhibitors.

2. Experimental

2.1. Reagents and materials

Hydrogen tetrachloroaurate trihydrate ($HAuCl4 \cdot 3H_2O$) and tri (2-carboxyethyl) phosphine hydrochloride (TCEP) were obtained from Aladdin (Shanghai, China). Dam MTase and Mbo I were supplied by New England Biolabs (Ipswich, MA). 6-Mercapto-1-hexanol (MCH), methylene blue hydrate (MB), bovine serum albumin (BSA, 99%) and 5-fluorouracil were purchased from Sigma-Aldrich (St. Louis, USA). All other reagents were of analytical reagent grade without further purification before use. Ultrapure water (Milli-Q 18.2 MΩ, Millipore System Inc.) was used for all the experiments.

All oligonucleotide sequences were synthesized by Shanghai Sangon Biotechnology Co. (Shanghai, China) and used without further purification. The base sequences of oligonucleotides were as following: DNA S1, 5′-SH-$(CH_2)_6$-GTA CAT CGT *GAT C*GC GAC GCG CTA CAG TCT TGA GCC-3′; DNA S2, 5′-GTC GC*G ATC* ACG ATG TAC-3′; DNA S3, 5′-SH-$(CH_2)_6$-GCC GGC TCA AGA CTG TAG-3′; single-based mismatch DNA S4, 5′-GTC GC*G AGC* ACG ATG TAC-3′. The recognition site for Dam MTase and Mbo I endonuclease were marked with italics.

2.2. Instrumentation

All electrochemical experiments were carried out using a CHI 660D electrochemical workstation (Shanghai Chenhua Instruments, China). A conventional three-component electrochemical cell was employed in all electrochemical measurements, with a modified Au electrode as the working electrode, a KCl-saturated Ag/AgCl electrode as a reference electrode and a Pt wire as the auxiliary electrode. UV–visible absorption spectroscopy (NANODROP1000 Spectrophotometer, Thermo, USA) and transmission electron microscopy (TEM, H600, Hitachi, Japan) were used to investigate the morphology of AuNPs and DNA S3-AuNPs.

2.3. Preparation of DNA S3-AuNPs bioconjugates

Gold nanoparticles (16 nm) were prepared according to a standard citrate method (Frens, 1973; Jin et al., 2003; Liu and Lu, 2006). Briefly, 50 mL of $HAuCl_4$ solution (0.01%, m/v) was boiled with vigorous stirring, and 2 mL of trisodium citrate solution (1%, m/v) was added quickly into the boiling solution. When the color of the solution changed from pale yellow to wine red, it indicated that the AuNPs were formed. After left stirring and cooled to room temperature, the resulting solution was stored in brown glass bottles at 4 °C for future use.

DNA S3 modified AuNPs were prepared according to the previously reported methods with slight modification (Liu and Lu, 2006). Before DNA loading on the AuNPs surface, thiolated modified DNA S1 was activated by treatment with 100-fold excess TCEP at room temperature for 1 h. Then, 15 μL, 100 μM DNA S3 was mixed with 500 μL AuNPs solution and incubated at 4 °C for 12 h. After incubation, 10 μL of 1% SDS was added to stabilize the AuNPs with shaking at room temperature for 1 h. Then the DNA S3-AuNPs were aged for 12 h by slowly adding 50 μL 0.5 M NaCl solution. To remove excess reagents, the solution was centrifuged at 12,000 rpm for 20 min. The wine red DNA S3-AuNPs precipitate was washed 3 times by centrifugation with 0.01 M phosphate buffer solution (pH 7.4) and then resuspended in 0.5 mL 2 × SSC hybridization buffer (30 mM sodium citrate, 300 mM NaCl) for future use.

2.4. Preparation of gold electrode

The gold electrode (3 mm diameter) was carefully polished to a mirror-like finish with alumina powder of 0.3 and 0.05 μm, followed by sequential sonication for 10 min each in ultrapure water, ethanol, and ultrapure water. Then it was dipped in freshly prepared piranha solution (98% H_2SO_4: 30% H_2O_2, 3:1 by volume) for 10 min and rinsed with ultrapure water thoroughly. The electrode was then scanned in 0.1 M H_2SO_4 between −0.2 V and 1.55 V at 100 mV/s until a reproducible cyclic voltammogram (CV) was obtained. Once completed, the electrode was washed with double distilled water and dried under nitrogen.

2.5. Immobilization of DNA S1 and hybridization

After pretreatment, the electrode was incubated with 10 μL of 1 μM DNA S1 solution (10 mM Tris–HCl and 1 mM EDTA, pH 8.0) for 12 h at 4 °C. To further eliminate the non-specifically immobilized DNA and obtain well-aligned DNA monolayers, 10 μL of 1 mM MCH solution and 10 μL of 1% BSA solution was successively dropped on the electrode surface and kept at room temperature for 1 h and 0.5 h, respectively. The hybridization was conducted by dropping 10 μL of 1 μM DNA S2 solution (30 mM sodium citrate, 300 mM NaCl) onto the electrode surface for 2 h at 37 °C. Subsequently, 10 μL of DNA S3-AuNPs bioconjugates were dropped onto the electrode surface for 2 h at 37 °C to hybridize the upper portion of DNA S1. After each step, the electrode was rinsed with washing buffer (20 mM Tris–HCl, 0.1 M NaCl, 5 mM $MgCl_2$) and dried with nitrogen.

2.6. Electrochemical detection of Dam MTase

For methylation, the electrode was incubated with 10 μL of different concentrations of Dam MTase solution, which was performed in Dam MTase reaction buffer (50 mM Tris–HCl, 5 mM 2-mercaptoethanol, 10 mM EDTA, pH 7.5) containing 80 μM SAM and a varying amount of Dam MTase at 37 °C for 2 h strictly. After methylation, the electrode was washed thoroughly with ultrapure water to terminate the methylation reaction according to some previously reported methods (Wang et al., 2013; Wang et al., 2012; Yin et al., 2013a, 2013b), and dried under nitrogen. Mbo I cleavage was performed at 37 °C for 2 h in Mbo I buffer (50 mM potassium acetate, 20 mM Tris–acetate, 10 mM magnesium acetate, 100 μg/mL BSA, pH 7.9) containing 50 U/mL Mbo I endonuclease. Thereafter the electrode was immersed in the 10 mL of 20 mM Tris–HCl buffer (pH 7.4) containing 20 μM MB and 20 mM KCl to equilibrate for 5 min before measurements. To obtain a stable and high signal, the differential pulse voltammetry (DPV) measurement was conducted in the presence of MB. Each electrochemical measurement was repeated at least 3 times under the same condition with the following parameters: initial potential, −0.50 V; final potential, 0.20 V; increment potential, 0.005 V; pulse amplitude, 0.05 s; pulse width, 0.05 s; sample width, 0.0167 s; pulse period, 0.5 s; and quite time, 2 s.

2.7. Influence of inhibitors on Dam MTase activity

The inhibition of drugs on Dam MTase activity could also be quantitatively analyzed using this method. A typical mixture contained Dam MTase (50 U/mL), methylation reaction buffer

(50 mM Tris–HCl, 5 mM 2-mercaptoethanol, 10 mM EDTA, pH 7.5), 80 μM SAMe and various concentrations of 5-fluorouracil. The process was similar to the assay of Dam MTase. Briefly, the electrode was treated with this mixture solution for 2 h at 37 °C, and then treated with Mbo I buffer (50 mM potassium acetate, 20 mM Tris–acetate, 10 mM magnesium acetate, 100 μg/mL BSA, pH 7.9) containing 50 U/mL Mbo I endonuclease for 2 h at 37 °C. Thereafter the electrode was rinsed thoroughly with ultrapure water. The current response was measured by DPV in 10 mL of 20 mM Tris–HCl buffer (pH 7.4) containing 20 μM MB and 20 mM KCl.

3. Results and discussions

3.1. Characterization

3.1.1. Characterization of AuNPs and DNA S3-AuNPs

The TEM and UV–vis absorption spectra were used to characterize the morphology of AuNPs and DNA S3-AuNPs. As shown in Fig. 1A, the TEM image of AuNPs indicated that the AuNPs obtained were spherical and the average size was about 16 nm. However, the TEM image of DNA S3 modified AuNPs was almost the same as AuNPs (Fig. 1B), and it was consistent with a previous report (Zhang et al., 2012). This could be ascribed to two reasons: first, the DNA S3 oligonucleotide is too short (sequence with only 18 bp) to characterize; second, for the characterization of number representation and probe state of DNA S3 on DNA S3-AuNPs bioconjugates, TEM analysis could not meet the ideal requirements. Therefore, we also employed UV–vis absorption spectra to characterize the AuNPs and DNA S3-AuNPs (Fig. 1C). Pure AuNPs showed a characteristic adsorption peak at 519 nm (spectrum 1). After being modified with thiolated DNA S3, the characteristic peak of AuNPs underwent a 5 nm red shift to 524 nm (spectrum 2), due to interparticle plasmon coupling. This was in accordance with other studies (X. He et al., 2011; Zhang et al., 2013). These results demonstrated the successful assembly of DNA S3 onto the AuNPs surface.

3.1.2. Electrochemical characterization of the biosensor

To verify the interface properties of the modified electrode, cyclic voltammetry (CV) was performed for each step of the

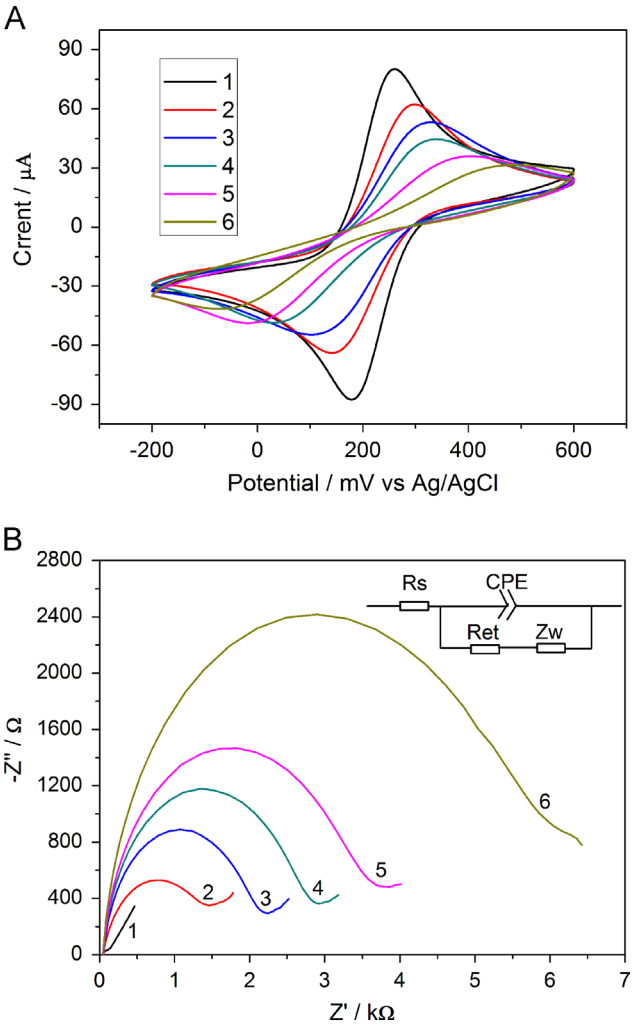

Fig. 2. Electrochemical characterization of the prepared biosensor. (A) Cyclic voltammetry and (B) Nyquist plots obtained from different electrodes in phosphate buffer solution (pH 7.0) containing 5 mM $[Fe(CN)_6]^{3-/4-}$ and 0.1 M KCl (scan rate of CV: 100 mV/s): (1) bare gold electrode; (2) DNA S1/Au; (3) MCH/DNA S1/Au; (4) BSA/MCH/DNA S1/Au; (5) DNA S2/BSA/MCH/DNA S1/Au; and (6) DNA S3-AuNPs/DNA S2/BSA/MCH/DNA S1/Au.

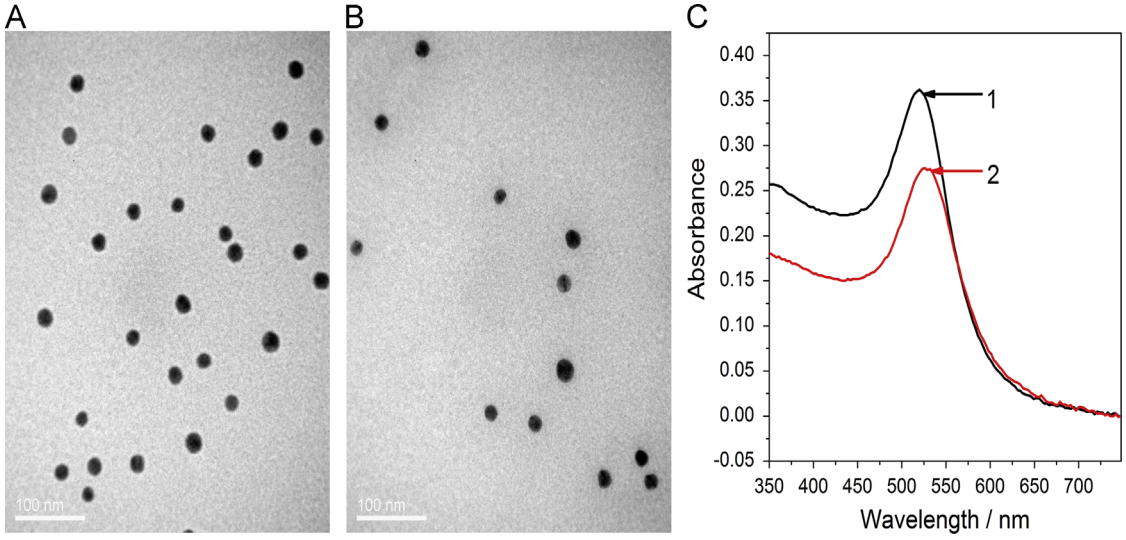

Fig. 1. TEM images of (A) AuNPs, (B) DNA S3-AuNPs, and (C) UV–vis absorption spectra of (spectrum 1) AuNPs and (spectrum 2) DNA S3-AuNPs.

working electrode preparation. As Fig. 2A shows, a well-defined redox pair was observed, showing a fast electron-transfer kinetics of $Fe(CN)_6^{3-/4-}$ on the bare gold electrode (curve 1). The current response decreased and the separation degree of two peaks was enlarged after the self-assembling process of DNA S1 (curve 2), caused by the electrostatic repulsion between the negatively charged deoxyribose-phosphate backbone of DNA S1 and $[Fe(CN)_6]^{3-/4-}$, indicating the successful immobilization of DNA S1. To eliminate the non-adsorbed DNA S1 molecules and hold a good orientation of DNA S1, MCH and BSA were, respectively, assembled onto the DNA S1 modified gold electrode, and large decrease in peak currents and enlarged peak-to-peak separation could be observed (curves 3 and 4). This could be related to the blocking effect of MCH and BSA to the permeation of redox species to the surface of the electrode. When hybridized with DNA S2, there was a further decrease of the redox current and further enlargement of peak separation (curve 5), resulted by the insulating behavior of duplexed DNA strands, implying the formation of a double helix structure of DNA S1 and DNA S2. After hybridization with DNA S3-AuNPs, the lowest redox peaks were obtained (curve 6) due to the inhibition effect on electron transfer when large molecules like DNA S3-AuNPs attached onto the surface, since a single AuNP could be loaded with a huge amount of DNA. Also, the space steric hindrance caused by the entrance of DNA S3-AuNPs composites through the hybridization between DNA S1 and DNA S3 also made some contribution to the decrease of the redox current peaks. All the CV data indicated the successful fabrication of the electrochemical biosensor.

Electrochemical impedance spectroscopy (EIS) was also used to monitor features of the modified gold electrode. The curve of EIS presented as the Nyquist plot consisted of two portions: one portion was the semicircle section at high frequencies related to the electron transfer limited process. The electron transfer resistance (R_{et}) could be obtained by measuring the diameter of semicircle. The other portion was a linear section at low frequencies corresponding to the diffusion-limited process held in solution. The electrolyte resistance was measured at low frequencies. The EIS data were fitted by an equivalent electrical circuit (inset, Fig. 2B). Fig. 2B shows a significant difference in the R_{et} obtained from each surface modification step. Bare gold electrode exhibited a small semicircle portion (curve 1) due to the free electron-transfer process. Increase in the R_{et} for the DNA S1 immobilized electrode (curve 2) revealed that DNA S1 hindered the electron transport from the solution to the electrode surface, suggesting the successful assemblage of DNA S1. Further increment in R_{et} value after the immobilization of MCH (curve 3) and BSA (curve 4), was attributed to the blocking of MCH and BSA with nonconductive properties, resulting in the reduction of electron transport flow. After the hybridization with DNA S2, a large increase in R_{et} was observed (curve 5) due to the formation of dsDNA which possessed a large amount of negatively charged deoxyribose-phosphate backbone, implying that DNA hybridization favorably occurred onto the electrode. When DNA S3-AuNPs composites attached onto the surface of the gold electrode through hybridization between DNA S1 and DNA S3, the R_{et} largely increased (curve 6); this increase clearly demonstrated the successful binding of DNA S3-AuNPs onto the electrode surface. The changes in EIS were in agreement with those in the CV method, which further demonstrated the success of each modification step.

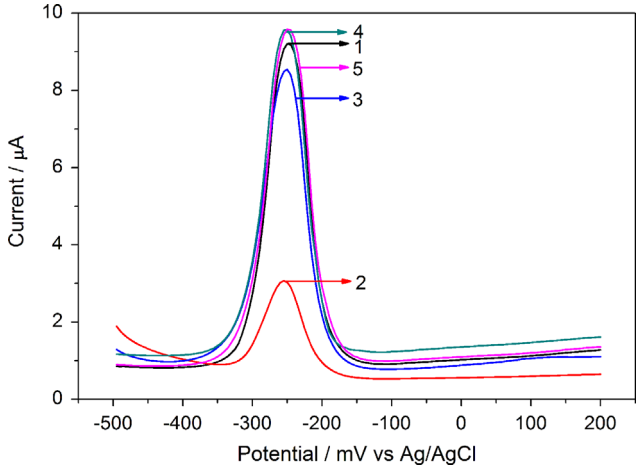

Fig. 3. Differential pulse voltammograms of (curve 1) the DNA S1/S2/S3-AuNPs modified gold electrode, (curve 2) the DNA S1/S2/S3-AuNPs modified gold electrode treated with Mbo I, (curve 3) the DNA S1/S2/S3-AuNPs modified gold electrode treated with Dam MTase and Mbo I, (curve 4) the DNA S1/S4/S3-AuNPs modified gold electrode treated with Mbo I, and (curve 5) the DNA S1/S4/S3-AuNPs modified gold electrode treated with Dam and Mbo I. All data were recorded in a 20 mM Tris–HCl buffer (pH 7.4) containing 20 μM MB and 20 mM KCl.

3.2. Feasibility and selectivity investigation of the electrochemical biosensor

Differential pulse voltammetry (DPV) was performed to investigate the feasibility of the electrochemical assay. As shown in Fig. 3, after both DNA S2 and DNA S3-AuNPs hybridized with DNA S1, methylene blue was accumulated as the electrochemical indicator and a well-defined current peak of MB appears at −250 mV (curve 1). A significant decrease of the electrochemical current signal was observed after the hybridization composites (unmethylated) were only treated with Mbo I endonuclease (50 U/mL) (curve 2), because Mbo I could specifically recognize the site of 5′-G-A-T-C-3′ and large amounts of DNA S3-AuNPs deviated from the surface of the electrode, less MB was adsorbed on hybridization composites. However, if the DNA S1/S2/S3-AuNPs composites were firstly methylated by Dam MTase (50 U/mL), then digested by Mbo I (50 U/mL), only a small decrease of the response of MB happened (curve 3), because most of the digestion effect by the Mbo I was blocked after the site of 5′-G-A-T-C-3′ was methylated to 5′-G-Am-T-C-3′ by Dam methyltransferase. It demonstrated that the site of 5′-G-A-T-C-3′ in the hybridization composite was successfully methylated by Dam MTase, and the Mbo I endonuclease would not cleave the DNA S1/S2/S3-AuNPs hybridization composites in the presence of Dam MTase. These results suggested that the electrochemical assay for Dam MTase activity could be effectively carried out.

We also evaluated the methylation specificity by one-base mismatched synthetic DNA S4. DNA S1 was hybridized with DNA S4 and DNA S3-AuNPs, and then only treated with Mbo I (50 U/mL). The peak current of MB was still high when S1/S4/S3-AuNPs hybridization composites (unmethylated) were cleaved by Mbo I (curve 4), and the signal was higher than that obtained at voltammograms 1, 2 and 3. Meanwhile, we found that the DPV signal was almost invariable compared to voltammogram 4 if the DNA S1/S4/S3-AuNPs hybridization composites were methylated by Dam (50 U/mL) before digested by Mbo I (50 U/mL) (curve 5). It was known that MB could interact with DNA. Although the formation of dsDNA can improve the electrostatic interaction between MB and the deoxyribose-phosphate backbone, the specific interaction between MB and guanine residues was greatly obstructed, because guanine residues were enwrapped in dsDNA. Therefore, less MB was adsorbed on dsDNA than that on single-stranded DNA (ssDNA). Although there were some single DNA S4 which did not hybridize with DNA S1 because of one-base mismatch, the current signal of DNA S1/S4/S3-AuNPs was higher than that obtained from DNA S1/S2/S3-AuNPs. It suggested that Mbo I had no effect on the DNA S1/S4/S3-AuNPs hybridization composites, because the hybrids did not contain a specific

recognition sequence (5′-G-A-T-C-3′) for the endonuclease Mbo I. These results implied that the interaction model of Dam MTase-Mbo I endonuclease could distinguish even one-base mismatched DNA and therefore could be applied to highly selective determination of Dam DNA methylation at the site of 5′-G-Am-T-C-3′.

3.3. Optimization of experimental conditions

Acted as the methylation donor, SAM played a crucial role in the process of DNA methylation catalyzed by Dam MTase, so the concentration of SAM was optimized in our assay. With the concentration of SAM increasing from 0 to 160 μM (Fig. S1A), the signal current increased gradually, and then slowly increased when the concentration of SAM exceeded 80 μM. As a result, 80 μM of SAM was employed for the sensing system in the following experiments.

Mbo I endonuclease could only cleave the sequence of 5′-G-A-T-C-3′ before the internal adenine methylated, which was important to the final current signal, so we investigated the effect of Mbo I concentration on the assay. As Fig. S1B shows, with the increasing concentrations of Mbo I, the current signal decreased and finally tended to a plateau phase at 50 U/mL. Thus, 50 U/mL of Mbo I was chosen for the following experiments.

3.4. Dam MTase detection

The current signal was directly related to the quantity of methylated duplex target sequence 5′-G-Am-T-C-3′, which was methylated by Dam MTase. For the detection of Dam MTase concentration, the DNA S1/S2/S3-AuNPs composites on the electrode surface were firstly methylated with Dam MTase for 2 h, and then cleaved with Mbo I endonuclease; finally, the current response of MB was recorded by DPV. We obtained a series of current signals by exposing the fabricated sensor to a series of Dam MTase concentrations under the same optimized experimental conditions. As shown in Fig. 4A, with Dam MTase's concentration changing from 0 to 60 U/mL, the current signal increased gradually. The results shown in the inset of Fig. 4B revealed a good linear relationship between the DPV peak currents and the logarithm of concentrations of the Dam MTase in the range of 0.075–30 U/mL, with a correlation coefficient (R) of 0.999. The regression equation could be expressed as $I(\mu A)=5.17782+2.08233\ \lg[C]$, where I is the peak current and C is the concentration of Dam MTase ($n=3$). The linear range of the proposed method (0.075–30 U/mL) was wider than some of previous reports based on electrochemical and colorimetric methods, such as 0.2–10 U/mL (Y. He et al., 2011), 1.0–10 U/mL (Liu et al., 2009), 0.25–10 U/mL (Wang et al., 2013), and 0.1–20 U/mL (Wu et al., 2012). The detection limit could be estimated as 0.02 U/mL based on the 3σ rule ($S/N=3$), which was rather lower, compared to some previous methods, such as 0.1 ± 0.02 U/mL (S. Liu et al., 2011), 0.08 U/mL (Jiang et al., 2012), and 0.06 U/mL (Zhao et al., 2013). This low detection limit indicated that a very low concentration of analyte could be detected using our proposed method. This could help to early diagnose the DNA MTase related diseases in theory. We could know from the slope of regression equation that a tiny variation of Dam concentration could result in a large signal change, which was more obvious than some previous reports (X. He et al., 2011; Wang et al., 2013). This demonstrated an excellent sensitivity of our proposed method. The satisfactory detection limit and sensitivity could be mainly ascribed to the signal amplification units DNA S3-AuNPs, which were employed to adsorb more MB molecules on the electrode surface. As a result, the detection signal was effectively amplified. More comparisons of our work with previously reported similar methodologies from some different aspects are shown in Table S1. It can be seen that our developed method could be used to detect DNA methylation and activity of Dam MTase simply, sensitively and effectively.

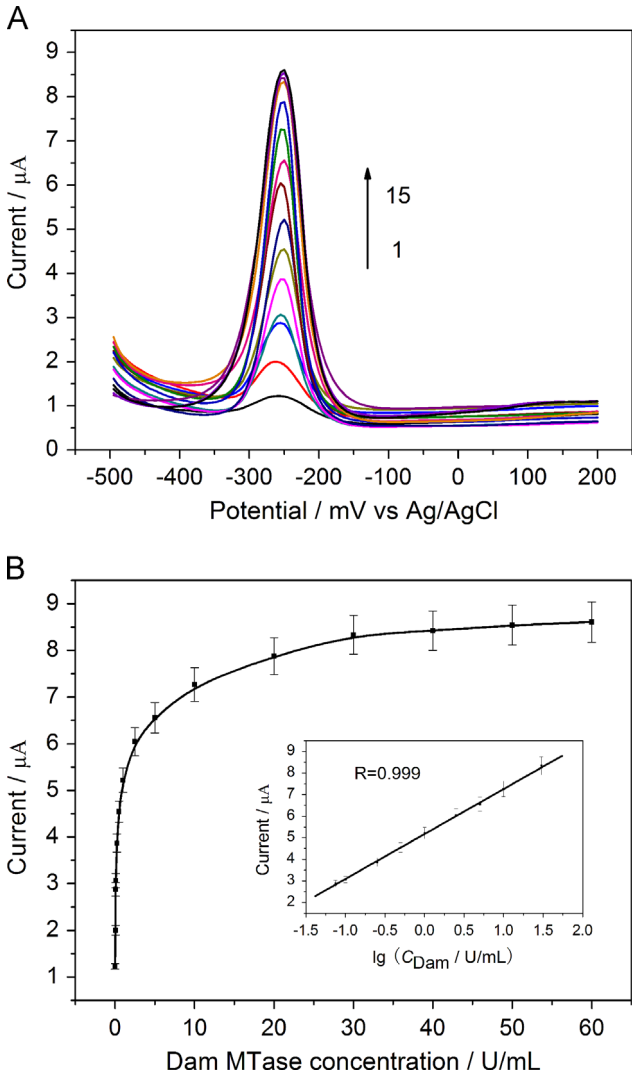

Fig. 4. (A) Differential pulse voltammograms for the modified electrodes. The DNA S1/S2/S3-AuNPs bioconjugates on the electrode were methylated by (1–15) 0, 0.05, 0.075, 0.1, 0.25, 0.5, 1, 2.5, 5, 10, 20, 30, 40, 50 and 60 U/mL Dam MTase and cleaved with 50 U/mL Mbo I. (B) The response voltammogram obtained with variable concentrations of Dam MTase from 0 to 60 U/mL. Error bars represent standard deviations of measurements ($n=3$). The inset shows a linear relationship between the peak currents and the logarithm of concentrations of Dam MTase from 0.075 to 30 U/mL.

3.5. The inhibition of 5-fluorouracil on the activity of Dam MTase

DNA methylation played an important role in both prokaryotes and eukaryotes. There was a correlation between DNA methylation and inactivation of various pathways involved in the tumorigenic process, including DNA repair (Li et al., 1993), cell cycle regulation (Li et al., 1992), inflammatory/stress response (Beard et al., 1995), and apoptosis (Esteller, 2002). The activity of DNA MTase, which catalyzed DNA methylation with SAM as the methyl donor, was crucial in this process. Thus, the pharmacological inhibitors of DNA MTase had promising applications for antibiotics and anticancer therapeutics. To further extend the potential application of this electrochemical sensor in screening MTase inhibitor, we investigated the influence of 5-fluorouracil on the activity of Dam MTase. As Fig. 5A shows, with the increasing concentrations of inhibitor 5-fluorouracil, the signal peak currents gradually decreased, and the relative activity of Dam

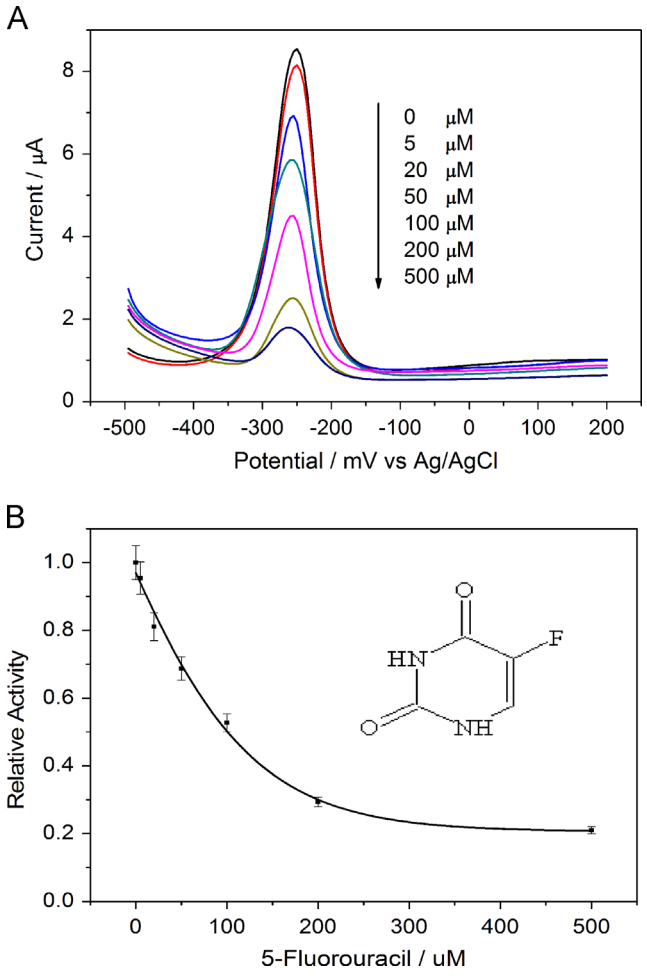

Fig. 5. Inhibition efficiency of Dam MTase by 5-fluorouracil. (A) Differential pulse voltammograms for different concentrations of 5-fluorouracil. The DNA S1/S2/S3-AuNPs bioconjugates on the electrode were treated with 0, 5, 20, 50, 100, 200, 500 μM 5-fluorouracil and 50 U/mL Dam MTase, then cleaved with 50 U/mL Mbo I. (B) The relative activity of Dam MTase after inhibited by different concentrations of 5-fluorouracil (0, 5, 20, 50, 100, 200, and 500 μM). Error bars represent standard deviations of measurements ($n=3$).

MTase decreased as well (Fig. 5B). Both of these results indicated that the Dam MTase activity was inhibited, which demonstrated that the fabricated sensor could be used to screen inhibitors of Dam MTase.

3.6. Precision, repeatability and stability of the electrochemical biosensor

In this study, the assay precision was assessed using the slopes of calibration plots obtained from three independent assay systems. The relative standard deviation (RSD) of the three slopes was 5.13%, which reflects a high precision. Owing to the fact that precision is the prerequisite condition of accuracy, the assay precision was higher, and the determination was closer to reality. This high precision indicated that the developed method could be applied to effectively analyze Dam MTase activity.

The repeatability of the proposed method was investigated by detecting 50 U/mL of Dam MTase using five independent freshly fabricated biosensors. The RSD was about 5.28%, implying an acceptable repeatability of the developed method, which may be ascribed to the stability of DNA-AuNPs composites. The acceptable repeatability demonstrated that if only we conduct the assay as the proposed procedure, we can obtain stable and coincident results. With this low inter-assay coefficient of variation, each determination can effectively reflect the activity of the Dam methyltransferase.

The stability of the fabricated biosensor was also investigated. When the fabricated sensor was stored in a refrigerator at 4 °C for 10 days, 90.46% of the initial response current was retained. This result suggested that the electrochemical biosensor had good stability. Our prepared biosensor has a relatively long quality guarantee period, and it can ensure the effectiveness and reliability of detection in a period time for practical application.

4. Conclusion

In summary, a sensitive and selective electrochemical biosensor for the detection of DNA methylation, assay of DNA MTase activity, and screening of inhibitors was successfully developed. Taking advantages of the amplification capability of DNA-AuNPs and the electroactivity of MB that combined with DNA through three modes of interaction, a relatively lower detection limit of 0.02 U/mL and a wider linear range from 0.075 to 30 U/mL were achieved. Compared to other electrochemical methods, our method was simple, selective and sensitive. Furthermore, the influence of the inhibitor 5-fluorouracil on the activity of Dam MTase was directly measured. In addition, the proposed analysis mode had improved generality and could be extended to the detection of other DNA MTase and the corresponding inhibitor screening by exchanging the corresponding DNA sequence, which had significant value to disease diagnosis and drug development associated with DNA methylation.

Acknowledgments

This work was financially supported by the Natural Science Research Foundation of China (81171415).

Appendix A. Supplementary material

Supplementary data associated with this article can be found in the online version at http://dx.doi.org/10.1016/j.bios.2014.02.035.

References

Adams, R., Rinaldi, A., Seivwright, C., 1991. J. Biochem. Biophys. Methods 22, 19–22.
Adams, R.L., 1990. Biochem. J. 265, 309–320.
Baek, S., Won, B.Y., Park, K.S., Park, H.G., 2013. Biosens. Bioelectron. 49, 542–546.
Baron, R., Willner, B., Willner, I., 2007. Chem. Commun. 4, 323–332.
Baylin, S.B., Ohm, J.E., 2006. Nat. Rev. Cancer 6, 107–116.
Beard, C., Li, E., Jaenisch, R., 1995. Genes Dev. 9, 2325–2334.
Bergerat, A., Guschlbauer, W., Fazakerley, G.V., 1991. Proc. Natl. Acad. Sci. 88, 6394–6397.
Boye, E., Marinus, M.G., Løbner-Olesen, A., 1992. J. Bacteriol. 174, 1682–1685.
Brueckner, B., Lyko, F., 2004. Trends Pharmacol. Sci. 25, 551–554.
Cao, Y., Yuan, R., Chai, Y., Mao, L., Niu, H., Liu, H., Zhuo, Y., 2012. Biosens. Bioelectron. 31, 305–309.
Chen, J., Zhang, J., Li, J., Fu, F., Yang, H.-H., Chen, G., 2010. Chem. Commun. 46, 5939–5941.
Chen, X., Zhang, K., Zhou, J., Xuan, J., Yan, W., Jiang, L.-P., Zhu, J.-J., 2010. Biosens. Bioelectron. 25, 1130–1136.
Dai, Z., Hu, X., Wu, H., Zou, X., 2012. Chem. Commun. 48, 1769–1771.
Eads, C.A., Danenberg, K.D., Kawakami, K., Saltz, L.B., Danenberg, P.V., Laird, P.W., 1999. Cancer Res. 59, 2302–2306.
Egger, G., Liang, G., Aparicio, A., Jones, P.A., 2004. Nature 429, 457–463.
Erdem, A., Kerman, K., Meric, B., Akarca, U.S., Ozsoz, M., 2000. Anal. Chim. Acta 422, 139–149.
Esteller, M., 2002. Oncogene 21, 5427–5440.
Frauer, C., Leonhardt, H., 2009. Nucleic Acids Res. 37, e22.
Frens, G., 1973. Nature 241, 20–22.
Grandjean, V., Yaman, R., Cuzin, F., Rassoulzadegan, M., 2007. PLoS One 2, e1136.
He, X., Su, J., Wang, Y., Wang, K., Ni, X., Chen, Z., 2011. Biosens. Bioelectron. 28, 298–303.

He, Y., Zhang, S., Zhang, X., Baloda, M., Gurung, A.S., Xu, H., Zhang, X., Liu, G., 2011. Biosens. Bioelectron. 26, 2018–2024.
Heithoff, D.M., Sinsheimer, R.L., Low, D.A., Mahan, M.J., 1999. Science 284, 967–970.
Holliday, R., 1987. Science 238, 163–170.
Horton, J.R., Liebert, K., Bekes, M., Jeltsch, A., Cheng, X., 2006. J. Mol. Biol. 358, 559–570.
Jeltsch, A., 2002. ChemBioChem 3, 274–293.
Jiang, C., Yan, C.-Y., Huang, C., Jiang, J.-H., Yu, R.-Q., 2012. Anal. Biochem. 423, 224–228.
Jie, G.-F., Liu, P., Zhang, S.-S., 2010. Chem. Commun. 46, 1323–1325.
Jin, R., Wu, G., Li, Z., Mirkin, C.A., Schatz, G.C., 2003. J. Am. Chem. Soc. 125, 1643–1654.
Jones, P.A., Baylin, S.B., 2002. Nat. Rev. Genet. 3, 415–428.
Katz, E., Willner, I., 2004. Angew. Chem. Int. Ed. 43, 6042–6108.
Kerman, K., Ozkan, D., Kara, P., Meric, B., Gooding, J.J., Ozsoz, M., 2002. Anal. Chim. Acta 462, 39–47.
Li, E., Beard, C., Jaenisch, R., 1993. Nature 366, 362–365.
Li, E., Bestor, T.H., Jaenisch, R., 1992. Cell 69, 915–926.
Li, W., Liu, Z., Lin, H., Nie, Z., Chen, J., Xu, X., Yao, S., 2010. Anal. Chem. 82, 1935–1941.
Lin, X.-H., Wu, P., Chen, W., Zhang, Y.-F., Xia, X.-H., 2007. Talanta 72, 468–471.
Liu, J., Lu, Y., 2006. Nat. Protoc. 1, 246–252.
Liu, K., Zhang, J.-J., Wang, C., Zhu, J.-J., 2011. Biosens. Bioelectron. 26, 3627–3632.
Liu, S., Wu, P., Li, W., Zhang, H., Cai, C., 2011. Chem. Commun. 47, 2844–2846.
Liu, T., Zhao, J., Zhang, D., Li, G., 2009. Anal. Chem. 82, 229–233.
Mashhoon, N., Pruss, C., Carroll, M., Johnson, P.H., Reich, N.O., 2006. J. Biomol. Screen. 11, 497–510.
Robertson, K.D., 2005. Nat. Rev. Genet. 6, 597–610.
Robertson, K.D., Wolffe, A.P., 2000. Nat. Rev. Genet. 1, 11–19.
Rosi, N.L., Mirkin, C.A., 2005. Chem. Rev. 105, 1547–1562.
Shames, D.S., Minna, J.D., Gazdar, A.F., 2007. Curr. Mol. Med. 7, 85–102.
Simon, R., 2005. J. Clin. Oncol. 23, 7332–7341.
Song, G., Chen, C., Ren, J., Qu, X., 2009. ACS Nano 3, 1183–1189.
Wan, Y., Wang, Y., Luo, J., Lu, Z., 2007. Biosens. Bioelectron. 22, 2415–2421.
Wang, G.L., Zhou, L.Y., Luo, H.Q., Li, N.B., 2013. Anal. Chim. Acta 768, 76–81.
Wang, M., Xu, Z., Chen, L., Yin, H., Ai, S., 2012. Anal. Chem. 84, 9072–9078.
Wu, H., Liu, S., Jiang, J., Shen, G., Yu, R., 2012. Chem. Commun. 48, 6280–6282.
Xu, Z., Wang, M., Zhou, T., Yin, H., Ai, S., 2013. Sens. Actuators B: Chem. 178, 412–417.
Yan, X.-J., Xu, J., Gu, Z.-H., Pan, C.-M., Lu, G., Shen, Y., Shi, J.-Y., Zhu, Y.-M., Tang, L., Zhang, X.-W., Liang, W.-X., Mi, J.-Q., Song, H.-D., Li, K.-Q., Chen, Z., Chen, S.-J., 2011. Nat. Genet. 43, 309–315.
Yin, H., Zhou, Y., Xu, Z., Chen, L., Zhang, D., Ai, S., 2013a. Biosens. Bioelectron. 41, 492–497.
Yin, H., Zhou, Y., Xu, Z., Wang, M., Ai, S., 2013b. Biosens. Bioelectron. 49, 39–45.
Yin, Z., Liu, Y., Jiang, L.-P., Zhu, J.-J., 2011. Biosens. Bioelectron. 26, 1890–1894.
Zhang, B., Liu, B., Tang, D., Niessner, R., Chen, G., Knopp, D., 2012. Anal. Chem. 84, 5392–5399.
Zhang, K., Tan, T., Fu, J.-J., Zheng, T., Zhu, J.-J., 2013. Analyst 138, 6323–6330.
Zhang, Y., Hu, N., 2007. Electrochem. Commun. 9, 35–41.
Zhao, Y., Chen, F., Wu, Y., Dong, Y., Fan, C., 2013. Biosens. Bioelectron. 42, 56–61.